Re-evaluation of CEB-FIP 90 prediction models for creep and shrinkage with experimental database

Zuanfeng Pan [a,*], ***Bing Li*** [b], ***Zhitao Lu*** [a]

[a] *School of Civil Engineering at Southeast University, Nanjing 210096, China*

[b] *School of Civil and Environmental Engineering at Nanyang Technological University, Singapore 639798, Singapore*

** Corresponding author. Tel.: +86 15050569180; fax: +86 2583793232. E-mail address: zfpan@ntu.edu.sg (Z. Pan).*

GRAPHICAL ABSTRACT

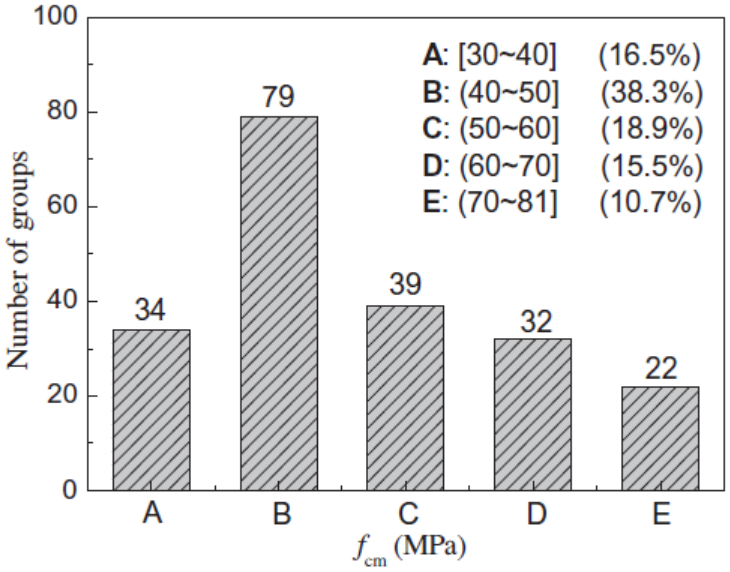

Distribution of f_{cm} of shrinkage database

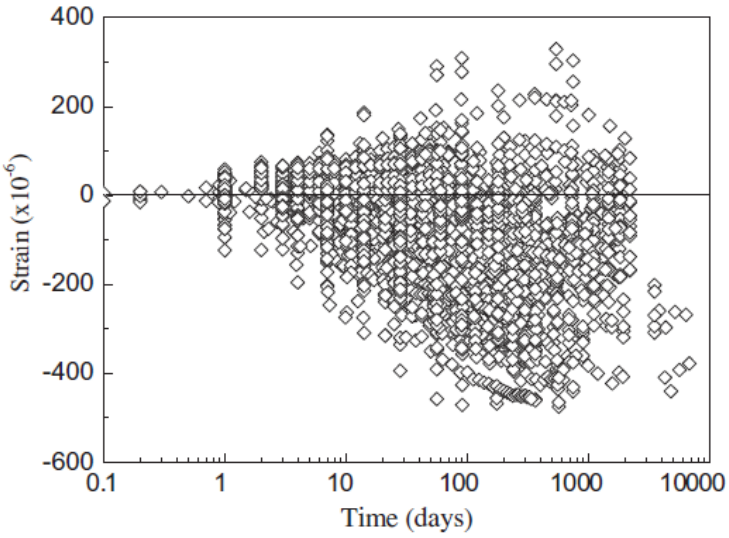

Shrinkage strain residuals for CEB-FIP90 model versus time

ABSTRACT

This paper aims to evaluate the CEB-FIP 90 model, which is commonly utilised to predict the creep and shrinkage effects of concrete structures, by comparing it with an extensive compiled database which combines the available data in literature and newly collected data from China. This database considers only concrete specimens with an average 28-day compressive strength between 30 MPa and 80 MPa, and restricts the relative humidity of the experimental environment to a maximum value of 95%. Three statistical methods are applied to evaluate the CEB-FIP 90 model: the residual method, the B3 coefficient of variation method, and the CEB coefficient of variation method. Based on the statistical regression analysis of the shrinkage and creep test data, the CEB-FIP 90 model is revised by modifying the influencing coefficients of the compressive strength of concrete and the time development functions of creep and shrinkage. The modified model is then subjected to evaluation and verification using the residual method, B3 coefficient of variation method and CEB coefficient of variation method. Based on verification with experimental data and corroboration with statistical analysis, the modified model performs better than CEB-FIP 90 model, especially with regards to high strength concrete.

1. Introduction

Creep and shrinkage of concrete are volume changes that develop over time, leading to the development of stresses, cracking and excessive deflections which compromise the long term serviceability and durability of concrete structures. Thus, it represents a key consideration in design, especially for the design of long-span prestressed concrete structures. This paper presents an evaluation of the existing CEB-FIP 90 model and aims to propose some improvements to increase the applicability and accuracy of its predictions. Creep and shrinkage are complex mechanisms involving a multitude of often interrelated factors, and there has been no theory as of yet that is able to satisfactorily explain the entire phenomenon. As such, experimental studies have served as the basis for creep and shrinkage models, and current models are largely based on empirical data and observations. Since the early 20th century, extensive experimental research has been conducted that has led to a variety of prediction models for creep and shrinkage. These models can be divided into three types. The first type of model describes the overall development of creep and includes CEB-FIP 90 [1], ACI 209-82 [2], AASHTO [3], GZ [4], and GL 2000 [5]; the second type of model divides creep into basic creep and drying creep, and includes BP-KX, BP-2, and B3 [6]; and the last type of model separates recovery creep from unrecoverable creep, such as CEB-FIP 78 [7].

However, recent years has seen the increased application of high strength concrete in concrete structures. Due to the dense microstructure of high strength concrete, its creep and shrinkage behaviour is markedly different from normal strength concrete. Most of the existing prediction models for creep and shrinkage are derived from the statistical regression analysis of test data, and data on normal-strength concrete account for a significant proportion of the available test data. As a result, the applicability of the existing prediction models to high strength concrete needs to be further evaluated, and there is also a need to generate a modified model based upon a new database incorporating more data on high strength concrete for use in engineering practice.

Currently, the widely adopted model for creep and shrinkage is the CEB-FIP 90 Model [1], which has been adopted in numerous concrete codes across the world such as the JTG D62-2004 [8]. Therefore this paper focuses on the evaluation of CEB-FIP 90 model, given its extensive application around the world.

The CEB-FIP 90 model is valid for concrete that has an average 28-day compressive strength in the range of 20 MPa to 90 MPa and an environmental relative humidity in the range of 40–100%, at a mean temperature of 5–30 ℃. The minimum compressive strength of concrete was set at 33 MPa in the compiled creep and shrinkage database for two reasons. First, the proportion of low-strength concrete will affect the applicability of the statistical regression model to high strength concrete; thus, a limited amount of extremely low-strength concrete was included in the database. Second, the creep and shrinkage of concrete play an important role in determining the long-term behaviours of long-span concrete structures, which are typically constructed with prestressed concrete. As specified in AASHTO [3], the compressive strength for prestressed concrete should not be lower than 28 MPa. In practice, however, the specified compressive strength for prestressed concrete usually exceeds 30 MPa. Therefore, a statistical evaluation of the CEB-FIP 90 model for concrete that has a compressive strength exceeding 30 MPa is imperative.

In comparison to previously established databases, such as those constructed by Bazant et al. [9,10] and Al-Manaseer and Lam [11], the present database is governed by three key distinguishing factors. First, the minimum compressive strength of concrete is limited to 33 MPa while other databases include numerous specimens with compressive strengths lower than 30 MPa. Second, experiments conducted in environments with 99% or 100% relative humidity are not considered, because these relative humidities only occur underwater. The range of environmental relative humidities considered in the database does not exceed 95%, which is the general maximum value for atmospheric humidity. Third, many experiments that were conducted in China were added to the database.

The compiled database is utilised to re-evaluate the CEB-FIP 90 model by the residual method, the B3 coefficient of variation method [12] and the CEB coefficient of variation method [13]. Furthermore, modified prediction models for creep and shrinkage that are based on the statistical regression analysis of the database are presented. The results of the statistical evaluation can provide the basic parameters for the uncertainty analysis of the effects of creep and shrinkage in concrete structures [14].

2. Experimental databases of creep and shrinkage

2.1. Experimental database of shrinkage

In total, 206 groups of specimens which were subjected to shrinkage tests were chosen for incorporation in the database, of which 48 groups were tested in China; this gives a total of 2838 data points [10, 15–22].

The distributions of the major parameters, namely the measured mean 28-day compressive strength of concrete, $f_{cm;}$ the environmental relative humidity, *RH*; and the effective thickness which accounts for the volume/surface ratio, *h* are shown in Fig. 1. It can be seen from Fig. 1 that 26.2% of the shrinkage specimens had a mean 28-day compressive strength in the range of 60–81 MPa, while the majority of concrete specimens had a mean compressive strength in the range of 30–60 MPa. In practice, the compressive strength of concrete that is widely used in prestressed concrete structures falls within the same strength range; hence, to some extent, the established database is representative of the shrinkage tendency of commonly used concrete. In this database, 91.7% of the shrinkage experiments were performed in an environment with relative humidity within the range of 40–80%, which is similar to the environmental conditions of actual concrete structures. Because the shrinkage experiments were performed under standard indoor environmental conditions, the effective thickness of the specimen was smaller than the thickness of the actual

concrete member. 93.7% of the specimens had an effective thickness in the range of 25 mm to 100 mm.

2.2. Experimental database of creep

In total, 179 groups of specimens originally devoted to creep tests (35 groups were conducted in China) have been selected to give a total of 3598 data points [10,15,18,19,23–25].

The distributions of the major parameters, namely $f_{cm,}$ RH, h, and τ are shown in Fig. 2. τ represents the concrete age at loading. It can be observed from Fig. 2 that 86.0% of the creep specimens had a mean 28-day compressive strength between 30 MPa and 60 MPa. In practice, the compressive strength of concrete that is widely used in prestressed concrete structures falls within the same strength range; hence, to some extent, the established database is representative of the creep tendency of commonly used concrete. In this database, the majority of the environmental relative humidities lie between 50% and 65%, which is similar to the actual structure environment. Similar to the shrinkage experiments, the creep experiments are carried out in a standard indoor environment, and the effective thickness of the specimen is smaller than the thickness of the actual concrete member. 93.9% of the specimens had an effective thickness in the range of 25–100 mm. In the database, the loading ages of creep specimens range from 5 days to 28 days, which accounted for 69.3% of the total specimens. For prestressed concrete bridges, the concrete age at loading generally exceeds 3 days; however, for long-span prestressed concrete bridges that are built via the cantilever construction method, the concrete age at loading ranges from 5 days to hundreds of days. The various stages of construction for long-span concrete bridges, such as post-tensioning, casting segments of bridge in-place, stretching the closure tendons, and deck paving, all utilise concrete with different loading ages. Hence, the database incorporated creep specimens with loading ages greater than 28 days (21.1% of the data).

3. Re-evaluation of the CEB-FIP 90 Model

The CEB-FIP 90 creep and shrinkage models are evaluated by using the aforementioned database. The predicted creep compliance (also known as creep function, which is the sum of the instantaneous elastic strain and the creep strain under unit uniaxial constant stress) and shrinkage strains in the model are compared with the test data that were extracted from the database. Three types of evaluation methods, the residual method (*RV*), the B3 coefficient of variation (ω_{B3}), and the CEB coefficient of variation (V_{CEB}) were applied to evaluate the prediction accuracy of the CEB-FIP 90 model.

When compared against the B3 coefficient of variation method and the CEB coefficient of variation method, the residual method appears relatively simple. The main underlying principle of the residual method is the subtraction of the predicted values from the measured values, followed by the analysis of the magnitude and distribution of the discrepancy. A positive difference implies that the model overestimated the shrinkage strain or creep compliance values. On the other hand, underestimation of the shrinkage strain or creep compliance values is reflected by a negative difference. To seek out the distribution of the residuals over time, the test data were categorised into three time ranges: 0–1000 days, 1001–9000 days and 0–9000 days. For further assessment, the residuals exceeding a certain microstrain (±100 $\mu\varepsilon$ for shrinkage and ±33 $\mu\varepsilon$/MPa for creep compliance) are classified to identify which model predicted values are closest to the test data. The Residual Value (*RV*) is calculated with the following equation:

$$RV = P - E \tag{1}$$

where *P* is the predicted value of the model and *E* is the measured value.

The B3 coefficient of variation method and the CEB coefficient of variation method were developed by Bazant and Baweja [12] and Muller and Hilsdorf [13]. Further

details of these two methods can be found in their papers [12,13].

3.1. Re-evaluation of the shrinkage model

The shrinkage strain residuals for the CEB-FIP 90 model versus time are shown in Fig. 3 and Table 1. A positive residual value implies that the model overestimates the experimental data, whereas a negative residual value indicates that the model underestimates the experimental values.

It is revealed from Fig. 3 and Table 1 that most of the shrinkage strain residuals fell on the negative side for short and long durations, which suggests that the model tended to underestimate the shrinkage strains. The overall distribution results of the data point residuals indicates that 73% of the residuals fell on the negative side while the remaining 27% of the residuals fell on the positive side.

The calculated ω_{B3} and V_{CEB} for the CEB-FIP 90 shrinkage model are 47.6% and 44.3%, respectively, and ω_{B3} was very close to the value (46%) obtained by Bazant and Baweja [12]. The CEB-FIP 90 shrinkage model considers the influence of the compressive strength of concrete, the environmental relative humidity and the effective thickness, whilst disregarding the impact of the composition of concrete. Therefore, the coefficients of variation of the predicted values by the CEB-FIP 90 shrinkage model are comparatively larger than the calculated value, which allows for the convenience of designers in engineering practice.

Most of the existing shrinkage and creep models are obtained through the statistical regression analysis of experimental data, which are mostly comprised of data from normal strength concrete specimens, making the model highly applicable to normal strength concrete rather than to high strength concrete. The shrinkage strain residuals for the CEB-FIP 90 model versus f_{cm} are shown in Fig. 4. As shown in Fig. 4, the residuals predicted by the CEB-FIP 90 model for specimens with compressive strength between 30 MPa and 40 MPa are distributed evenly on the positive and neg-

ative sides. However, for specimens with compressive strength above 40 MPa, the number of residuals that fall on the negative side is significantly larger than that falling on the positive side. The results corroborate with the previous observation that the CEB-FIP 90 model underestimates the shrinkage strain of high strength concrete. If the CEB-FIP 90 model is applied to high strength concrete structures, there is the potential for the serviceability of the structure to be undermined. Hence, the database confirms that there is a need to modify the influencing factors of the compressive strength of concrete, as specified in the CEB-FIP 90 model, to improve their accuracy in the prediction of shrinkage.

3.2. Re-evaluation of the creep model

The residuals of creep compliance for the CEB-FIP 90 model versus time are shown in Fig. 5 and Table 2. Positive values imply that the model overestimates the experimental values. Conversely, negative values indicate that the model underestimates the experimental data.

It can be observed from Fig. 5 and Table 2 that more than half of the total data points of creep compliance residuals fall on the positive side, for short and long durations. The overall distribution results of creep compliance residuals of data points indicate that 58% of the residuals fall on the positive side and 42% fall on the negative side. This finding indicates that the CEB-FIP 90 model slightly over-estimates the tested creep compliance. Furthermore, 93% of the residuals fall between 0 and ±33 $\mu\varepsilon$/MPa for 0–1000 days, and 90% of the residuals fall between 0 and ±33 $\mu\varepsilon$/MPa for 1001–9000 days. The calculated ω_{B3} and V_{CEB} for the CEB-FIP 90 creep model are 28.0% and 27.5%, respectively. Because many creep specimens that were collected in environments with a *RH* = 99% and 100% have been omitted, the calculated ω_{B3} is smaller than the value (35%) that Bazant and Baweja [12] concluded.

There is a discrepancy between the results shown in Table 2 and the results obtained by Al-Manaseer and Lam [11], who concluded that the CEB-FIP 90 model underestimated the creep compliance. There are two major factors that account for the discrepancy. The first reason is that specimens with low strength, such as with f_{cm} = 20–90 MPa, were collected [11]. Hence, the CEB-FIP 90 creep model is likely to underestimate the creep compliance of normal-strength concrete and especially of low-strength concrete. The second reason is that the database compiled by Al-Manaseer and Lam [11] incorporated the creep specimens that were collected in environments where *RH* = 99% and 100%; however, the CEB-FIP 90 model generally underestimated the creep compliance of concrete in environments with *RH* = 99% or 100%. If 166 groups of experimental data (3235 data points [10]) in environments where *RH* = 99% or 100% are added to the creep database, the residuals of creep compliance of the CEB-FIP 90 model are shown in Fig. 6. In Fig. 6, there are a total of 345 groups of creep specimens which gives a total of 6833 data points.

As depicted in Fig. 6, 44% of the residuals fall on the positive side and 56% of the residuals fall on the negative side. These results indicate that the CEB-FIP 90 model underestimates the creep compliance, which is contrary to the results that are depicted in Fig. 5. In as-built prestressed concrete structures, environments with *RH* = 99% or 100% are almost impossible to achieve. Hence, disregarding the creep specimens in environments where *RH* = 99% or 100% will better serve to reveal the creep characteristic of actual concrete structures.

The relationship between the creep compliance residuals for the CEB-FIP 90 model and the mean 28-day compressive strength of concrete is shown in Fig. 7. Along the axis of $f_{cm,}$ the residuals are uniformly distributed over the positive and negative sides. Therefore, the influencing coefficient of the compressive strength, as specified in the CEB-FIP 90 model, could represent the change in creep compliance of various concrete strength grades.

4. Modification and evaluation of creep and shrinkage models

4.1. Modified shrinkage model

It can be observed from Fig. 4 that the shrinkage strain residuals of the CEB-FIP 90 model are non-uniformly distributed over the positive and negative sides of the compressive strength. For specimens with compressive strength above 40 MPa, the residuals on the negative side are significantly greater than the residuals on the positive side. This finding indicates that the CEB-FIP 90 model underestimates the shrinkage strain for high strength concrete. Therefore, the strength coefficient, $\mathcal{E}_s$ (f_{cm}), of the shrinkage model should be modified. $\mathcal{E}_s$ (f_{cm}) of the shrinkage model can be calculated with the following equation:

$$\varepsilon_s(f_{cm}) = [160 + 10\beta_{sc}(9 - f_{cm}/f_{cm0})] \times 10^{-6} \tag{2}$$

where β_{sc} is the coefficient that describes the type of cement and is equal to 5.0 for normal Portland-type cement or rapid hardening cement; and f_{cm0} is equal to 10 MPa. Using the form of the CEB-FIP 90 shrinkage model, the following modified shrinkage model is proposed:

$$\varepsilon_{cs}(t, t_s) = [160 + 10\beta_{sc} \cdot \gamma(f_{cm})]\beta_{RH}\left[\frac{(t - t_s)/t_1}{350(h/h_0)^2 + (t - t_s)/t_1}\right]^{\alpha(f_{cm})} \tag{3}$$

where $\gamma(f_{cm})$ is the correction coefficient for the influence of f_{cm} and aimed at modifying the nominal shrinkage coefficient; t_s is the concrete age of curing; and h_0 is equal to 100 mm. In the CEB-FIP 90 model, $\gamma(f_{cm})$ = 9 − f_{cm}/f_{cm0} and a(f_{cm}) is the correction coefficient for the time development function, aimed at modifying the rate of shrinkage strain development with time. In the CEB-FIP 90 shrinkage model, $\alpha(f_{cm})$ is equal to 0.5.

Pertaining to Eq. (3) and by taking the logarithm of both sides, the following equation is obtained:

$$\ln[\varepsilon_{cs}(t,t_s)] = \ln\{[160 + 10\beta_{sc}\cdot\gamma(f_{cm})]\beta_{RH}\} + \alpha(f_{cm}) \times \ln\left[\frac{(t-t_s)/t_1}{350(h/h_0)^2 + (t-t_s)/t_1}\right] \quad (4)$$

Assuming $y = \ln[\varepsilon_{cs}(t,t_s)]$ and $x = \ln\left[\frac{(t-t_s)/t_1}{350(h/h_0)^2+(t-t_s)/t_1}\right]$, Eq. (4) is transformed into the form of $y = A + Bx$. By applying the linear least-squares method and regression analysis to each experimental group, the correction coefficient for the influence of f_{cm}, $\gamma(f_{cm})$, and the correction coefficient for the time development function, $\alpha(f_{cm})$ are determined. After regression analysis is performed for 206 groups of shrinkage specimens, the relationships between $\gamma(f_{cm})$ and f_{cm}, $\alpha(f_{cm})$ and f_{cm} are obtained. Linear fitting is then applied to the results, as shown in Fig. 8 and Fig. 9.

After appropriate simplification of the regression coefficient, the modified shrinkage model is developed as shown below:

$$\varepsilon_{cs}(t,t_s) = \varepsilon_{cs0}\beta_s(t-t_s) = \varepsilon_s'(f_{cm})\beta_{RH}\beta_s'(t-t_s) \quad (5)$$

$$\varepsilon_s'(f_{cm}) = [160 + 10\beta_{sc}(8.2 - 0.5f_{cm}/f_{cm0})]\times 10^{-6} \quad (6)$$

$$\beta_{RH} = 1.55[1-(RH/RH_0)^3] \quad (7)$$

$$\beta_s'(t-t_s) = \left[\frac{(t-t_s)/t_1}{350(h/h_0)^2 + (t-t_s)/t_1}\right]^{(0.64-0.02f_{cm}/f_{cm0})} \quad (8)$$

where RH_0 is equal to 100%. The comparison between the value of $\varepsilon_s'(f_{cm})$ in the modified model and the value of $\varepsilon_s(f_{cm})$ in the CEB-FIP 90 shrinkage model is shown in Fig. 10. The results in Fig. 10 demonstrate that the value of $\varepsilon_s'(f_{cm})$ is greater than the value of $\varepsilon_s(f_{cm})$. The expressions of $\varepsilon_s'(f_{cm})$ and $\varepsilon_s(f_{cm})$ suggest that

the ultimate shrinkage strain will decrease with an increase in the compressive strength of concrete. However, it is observed from Fig. 4 that an increase in compressive strength will cause the predicted accuracy of the CEB-FIP 90 shrinkage model to decrease. This finding indicates that the influence of the strength coefficient in the CEB-FIP 90 shrinkage model reduces the shrinkage strain to such an extent that it overestimates the reduction in real shrinkage. After the model is modified, the reduction correction coefficient increases. Hence, the modified model provides a better representation of the relationship between the ultimate shrinkage strain and the compressive strength of concrete. The comparison of the value of $\alpha(f_{cm})$ in the modified model and the value of $\alpha(f_{cm})$ (equals to 0.5) in the CEB-FIP 90 model is illustrated in Fig. 11. The exponent $\alpha(f_{cm})$ of the time development function of shrinkage mainly affects the development rate of shrinkage and has no effect on the ultimate shrinkage strain. The smaller the magnitude of the exponent $\alpha(f_{cm})$ is, the quicker the development of the early-phase shrinkage. As shown in Fig. 11, the magnitude of $\alpha(f_{cm})$ in the modified model decreases with an increase in the compressive strength of concrete. The rate of shrinkage development increases with an increase in the compressive strength of concrete, which is consistent with the conclusion of Huo [26].

4.2. Evaluation of the modified shrinkage model

The predicted shrinkage strain residuals of the modified shrinkage model with respect to time are shown in Fig. 12 and Table 3, and the shrinkage strain residuals versus the mean 28-day compressive strength of concrete are shown in Fig. 13.

As seen in Fig. 12 and Table 3, the distribution of residuals in the time range of 0–9000 days shows that 60% of the residuals fall on the negative side while the remaining 40% of the residuals fall on the positive side. This finding indicates that the model underestimated the shrinkage strain a little, especially during the time period of 0–1000 days. During the time period of 1001–9000 days, the residuals on both sides are almost uniformly distributed, with 53% positive values and 47% negative values.

It can be seen from Fig. 13 that the residuals of shrinkage strain versus f_{cm} are uniformly distributed on the positive and negative sides. Therefore, the strength coefficient in the modified model better reflects the change of shrinkage strain with respect to f_{cm}. The calculated ω_{B3} and V_{CEB} of the shrinkage strains predicted by the modified shrinkage model are 45.1% and 43.0%, respectively. The coefficients of variation in the modified model remain large as the same factors influencing shrinkage are considered as in the CEB-FIP 90 model; however, the modified model performs better than the CEB-FIP 90 model, especially with regards to high strength concrete.

4.3. Modified creep model

The approach used in the modification of the creep model is similar to the approach used in the modification of the shrinkage model. The correction coefficient for the compressive strength, $\beta'(f_{cm})$, aimed at modifying the nominal creep coefficient, and the correction coefficient for the time development function, $\gamma\,(f_{cm})$, aimed at modifying the rate of creep development with respect to time, are used in the modified creep model. The original $\beta(f_{cm})$ in the CEB-FIP 90 model is displayed below:

$$\beta(f_{cm}) = \frac{5.3}{(f_{cm}/f_{cm0})^{0.5}} \tag{9}$$

Using the form of the CEB-FIP 90 creep model, the modified creep model is proposed by the following equation:

$$\varphi(t,\tau) = \phi_{RH}\beta(\tau)\beta'(f_{cm})\left[\frac{(t-\tau)/t_1}{\beta_H + (t-\tau)/t_1}\right]^{\lambda(f_{cm})} \tag{10}$$

where t_1 is equal to 1 day. In the CEB-FIP 90 model, $\gamma(f_{cm})$ is equal to 0.3.

Pertaining to Eq. (10), and by taking the logarithm of both sides, the following equation is obtained:

$$\ln[\varphi(t,\tau)] = \ln[\phi_{RH}\beta(\tau)\beta'(f_{cm})] + \lambda(f_{cm})\ln\left[\frac{(t-\tau)/t_1}{\beta_H + (t-\tau)/t_1}\right] \tag{11}$$

Under the assumption that $y = \ln[\varphi(t,\tau)]$ and $x = \ln[\frac{(t-\tau)/t_1}{\beta_H+(t-\tau)/t_1}]$, Eq. (11) is transformed into the form $y = A + Bx$. By applying the linear least-squares method and regression analysis to each experimental group, $\beta'(f_{cm})$ and $\lambda(f_{cm})$ for each experimental group are determined. Through the regression analysis conducted on the 179 groups of creep experiments, the relationships between $\beta'(f_{cm})$ and f_{cm}, $\lambda(f_{cm})$ and f_{cm} are determined. Linear fitting is then applied to the results as shown in Fig. 14 and Fig. 15.

It can be observed from Fig. 15 that the exponent $\lambda(f_{cm})$ of the time development function remains almost constant with f_{cm}; as a result, it is selected as a mean value of 0.32 (greater than the exponential value of 0.3 in the original model). After the simplification of the regression coefficient, the following modified creep model is obtained:

$$\varphi(t,\tau) = \varphi_0\beta_c(t,\tau) = \varphi_{RH}\beta'(f_{cm})\beta(\tau)\beta_c'(t-\tau) \tag{12}$$

$$\varphi_{RH} = 1 + \frac{1 - RH/RH_0}{0.46(h/h_0)^{\frac{1}{3}}} \tag{13}$$

$$\beta'(f_{cm}) = \frac{6}{(f_{cm}/f_{cm0})^{0.6}} \tag{14}$$

$$\beta(\tau) = \frac{1}{0.1 + (\tau/t_1)^{0.2}} \tag{15}$$

$$\beta_c'(t-\tau) = \left[\frac{(t-\tau)/t_1}{\beta_H + (t-\tau)/t_1}\right]^{0.32} \tag{16}$$

$$\beta_H = 150\left[1 + \left(1.2\frac{RH}{RH_0}\right)^{18}\right]\frac{h}{h_0} + 250 \leqslant 1500 \quad (17)$$

A comparison of the value of $\beta'(f_{cm})$ in the modified model and the value of $\beta(f_{cm})$ in the CEB-FIP 90 model is shown in Fig. 16. An increase in the compressive strength results in a decrease in $\beta'(f_{cm})$ and $\beta(f_{cm})$. When f_{cm} is close to 30 MPa, the value of $\beta'(f_{cm})$ in the modified model and the value of $\beta(f_{cm})$ in the original model are approximately equal. An increase in the compressive strength yields a slightly lower value of $\beta'(f_{cm})$ in the modified model when compared with the original model.

4.4. Evaluation of the modified creep model

The results are summarised in Fig. 17 and Table 4. The number and percentage distribution of residual points for the modified creep model as a function of time are demonstrated in Table 4, and the number and percentage distribution of the residuals in various ranges for creep compliance as a function of accuracy range are also provided in Table 4. For short (0–1000 days) or long (1001–9000 days) time ranges, the residuals of the creep compliance are almost uniformly distributed on the positive and negative sides. Overall, 52% of the residuals are distributed on the positive side and 48% of the residuals fall on the negative side.

The results of Table 4 illustrate that 93% of the residuals are in the range of 0 to ±33 $\mu\varepsilon$/MPa for the 0–1000 days range, and 87% of the residuals are in the range of 0 to ±33 $\mu\varepsilon$/MPa for the 1001–9000days range. Hence, the modified model better represents creep. The calculated ω_{B3} and V_{CEB} of the creep compliance for the modified creep model are 26.6% and 26.9%, respectively.

The relationship between the residuals of creep compliance and f_{cm} is illustrated in Fig. 18. The residuals are uniformly distributed on the positive and negative sides, which indicates that $\beta'(f_{cm})$ in the modified creep model better reflects the change of creep compliance with respect to f_{cm}.

5. Conclusion

Most of the available prediction models for creep and shrinkage are derived through the statistical regression analysis of test data drawn mostly from experiments performed on normal strength concrete. While compiling the experimental data of creep and shrinkage for the statistical regression analysis, it is found that the percentage of the test data for various concrete strength grades affects the accuracy of prediction for the creep compliance and shrinkage strain for those specific strength grades of concrete. In this paper, extensive creep and shrinkage test data were collected. The present database features three salient characteristics, which consider the fact that the concrete strength grade that is used in actual concrete structures which are sensitive to creep and shrinkage, is usually greater than 30 MPa and that the environmental relative humidity rarely exceeds 95%. First, the database reflects an increase in data that were collected from experiments performed in China. Second, the minimum compressive strength of concrete utilised in the database was 33 MPa. Third, specimens were subjected to a maximum environmental relative humidity of 95%.

The residual method, the B3 coefficient of variation method and the CEB coefficient of variation method are used to evaluate the CEB-FIP 90 model with the database. The results of residual analysis indicate that the CEB-FIP 90 shrinkage model tends to strongly underestimate the shrinkage strain. Of the shrinkage data point values in the overall time range of 0–9000 days, CEB-FIP 90 model underestimates the shrinkage strain by 73% and overestimates the shrinkage strain by 27%. Especially for shrinkage specimens with f_{cm} above 40 MPa, the residuals that fall on the negative side are greater than the residuals that fall on the positive side, which indicates that CEB-FIP 90 model significantly underestimates the shrinkage strain of high strength concrete. CEB-FIP 90 model slightly overestimates the creep compliance and the percentage of data points underestimated and overestimated by the measured values of 42% and 58%, respectively. The calculated ω_{B3} and V_{CEB} of the shrinkage strains predicted by the CEB-FIP 90 model are 47.6% and 44.3%,

respectively, and the calculated ω_{B3} and V_{CEB} of the creep compliance for the CEB-FIP 90 model are 28.0% and 27.5%, respectively.

Based on the regression analysis of the experimental creep and shrinkage database, the CEB-FIP 90 model is modified, and then evaluated with the three aforementioned statistical methods. The results of residual analysis indicate that the modified shrinkage model slightly underestimates the shrinkage strain. However, the shrinkage strain residuals for the modified model are uniformly distributed on the positive and negative sides versus the compressive strength of concrete, which suggests that the modified shrinkage model is applicable to high strength concrete. The calculated ω_{B3} and V_{CEB} of the shrinkage strains predicted by the modified model are 45.1% and 43.0%, respectively. The percentage of data points which are underestimated and overestimated from the test values in the modified creep model are 48% and 52%, respectively. The calculated ω_{B3} and V_{CEB} of the creep compliance for the modified model are 26.6% and 26.9%, respectively. Based on verification with experimental data and corroboration with statistical analysis, the modified model performs better than the CEB-FIP 90 model, especially with regards to high strength concrete. However, the coefficients of variation in the model remain large as the same factors influencing creep and shrinkage are considered as in the CEB-FIP 90 model.

References

[1] Comité Euro-International Du Béton (CEB). CEB-FIP model code for concrete structures. Lausanne, Switzerland; 1990.

[2] American Concrete Institute (ACI). Prediction of creep, shrinkage and temperature effects in concrete structures, ACI-209R-82. ACI Committee 209. Detroit; 1982.

[3] American Association of State Highway and Transportation Officials (AASHTO). AASHTO LRFD bridge design specifications. 4th ed. Washington (DC); 2007.

[4] Gardner NJ, Zhao JW. Creep and shrinkage revisited. ACI Mater J 1993;90(3):236–46.

[5] Gardner NJ, Lockman MJ. Design provisions for drying shrinkage and creep of normal-strength concrete. ACI Mater J 2001;98(2):159–67.

[6] Bazant ZP, Baweja S. Creep and shrinkage prediction model for analysis and design of concrete structures: Model B3. Mater Struct 1995;28(180):357–65.

[7] CEB-FIP. Model code for concrete structures. Paris; 1978.

[8] JTG D62-2004. Code for design of highway reinforced concrete and prestressed concrete bridges and culverts. Peking; 2004.

[9] Bazant ZP, Li G. Unbiased statistical comparison of creep and shrinkage prediction models. Structural engineering report no. 07-12/A210u. Department of civil and environmental engineering. Northwestern University; 2007.

[10] Bazant ZP, Li G. Comprehensive database on concrete creep and shrinkage. Structural engineering report no. 08-3/A210c. McCormick school of engineering and applied science. Northwestern University; 2008.

[11] Al-Manaseer A, Lam JP. Statistical evaluation of shrinkage and creep models. ACI Mater J 2005;102(3):170–6.

[12] Bazant ZP, Baweja S. Justification and refinements of model B3 for concrete creep and shrinkage 1. Statistics and sensitivity. Mater Struct 1995;28(181):415–30.

[13] Muller HS, Hilsdorf HK. Evaluation of the time-dependent behavior of concrete, summary report on the work of general task group 9. CEB Bulletin d'

Information, No. 199; 1990.

[14] Pan Z, Fu CC, Jiang Y. Uncertainty analysis of creep and shrinkage effects in long-span continuous rigid frame of Sutong Bridge. J Bridge Eng, ASCE 2011;16(2):248–58.

[15] Meng S, Guan Y, Zhou X. Creep and shrinkage effects in the continuous rigid frame of Sutong Bridge. Report No. 05Y02. Research plan of transportation science in jiangsu province. Nanjing, China: Southeast University; 2007 [in Chinese].

[16] Ouyang H, Bai Y. Test study of shrinkage and creep behavior of high performance concrete. Bridge Construct 2006(2):4–6 [in Chinese].

[17] Zhou J. Study and application of C60 high performance concrete in Dubu No. 3 Bridge. Master's thesis. Department of materials science and engineering. Chongqing, China: Chongqing Jiaotong University; 2009 [in Chinese].

[18] Qin H, Pan G, et al. Study on deformation performance of high performance fly ash concrete used in Bridge Engineering. In: 11st National conference on concrete and prestressed concrete. Guiyang; 2001. p. 187–193 [in Chinese].

[19] Mu R, et al. Experimental study on mix design of high strength high performance concrete used in Sutong Bridge. Research Report. Nanjing, China: Jiangsu Research Institute of Building Science Co. Ltd.; 2005 [in Chinese].

[20] Wang G. Experiment of creep and shrinkage of concrete used in Paksey Bridge. Bengal. Research report. Wuhan, China: China Railway Major Bridge Engineering Group Co. Ltd.; 2003 [in Chinese].

[21] Chen C, Huang W, et al. Creep of high performance concrete for bridges and its application. Hydro-Science and Engineering 2007(2):1–9 [in Chinese].

[22] Li J. Study on impacts of weight fractions of limestone powder on properties of concrete. Master's thesis. Department of civil engineering. Dalian, China: Dalian University of Technology; 2007 [in Chinese].

[23] Chen L. Study on C60 low creep concrete. Master's thesis. Department of civil engineering. Changsha, China: Central South University; 2008 [in Chinese].

[24] Xie C. Experimental study on creep deformation of long-span bridge with ballastless track. Sci Technol West China 2009;8(7):26–7 [in Chinese].

[25] Xu J. Experimental and theoretical study on creep and shrinkage effects in continuous concrete bridges. Master's thesis. Department of bridge and tunnel engineering. Chongqing, China: Chongqing Jiaotong University; 2008 [in Chinese].

[26] Huo X. Time-dependent analysis and application of high performance concrete in bridges. PHD thesis. Department of civil engineering. Nebraska, USA: University of Nebraska; 1997.

List of Tables

List of Figures

Periods		0–1000 days	1001–9000 days	0–9000 days
Residuals	Data points	2660	178	2838
	Overestimate“ + ”	728(27%)	35(20%)	833(27%)
	Underestimate “–”	1932(73%)	143(80%)	2085(73%)
	0∼±100 $\mu\varepsilon$	1553(58%)	101(57%)	1654(58%)
	Exceeding ±100 $\mu\varepsilon$	1107(42%)	77(43%)	1184(42%)

Table 1

Periods		0–1000 days	1001–9000 days	0–9000 days
Residuals	Data points	3353	245	3598
	Overestimate“ + ”	1960(58%)	135(55%)	2095(58%)
	Underestimate “–”	1393(42%)	110(45%)	1503(42%)
	0∼ ± 33 $\mu\varepsilon$/MPa	3125(93%)	220(90%)	3345(93%)
	Exceeding ±33 $\mu\varepsilon$/MPa	228(7%)	25(10%)	253(7%)

Table 2

Periods		0–1000 days	1001–9000 days	0–9000 days
Residuals	Data points	2660	178	2838
	Overestimate“ + ”	1043(39%)	95(53%)	1138(40%)
	Underestimate “–”	1617(61%)	83(47%)	1700(60%)
	0∼ ± 100 $\mu\varepsilon$	1729(65%)	99(56%)	1828(64%)
	Exceeding ±100 $\mu\varepsilon$	931(35%)	79(44%)	1010(36%)

Table 3

Periods		0–1000 days	1001–9000 days	0–9000 days
Residuals	Data points	3353	245	3598
	Overestimate“ +”	1756(52%)	124(51%)	1880(52%)
	Underestimate “–”	1597(48%)	121(49%)	1718(48%)
	0∼ ± 33 $\mu\varepsilon$/MPa	3111(93%)	214(87%)	3325(92%)
	Exceeding ±33 $\mu\varepsilon$/MPa	242(7%)	31(13%)	273(8%)

Table 4

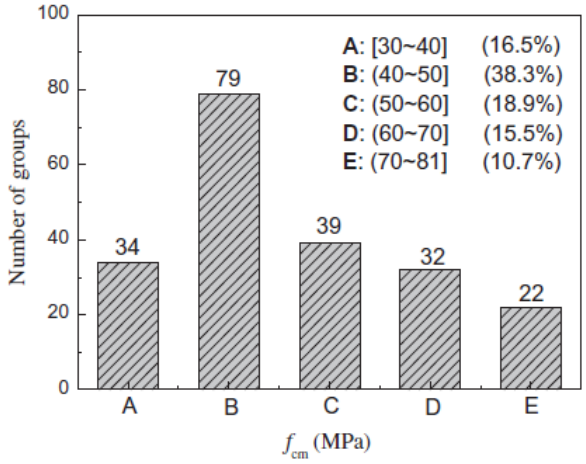

(*a*) Average 28-day compressive strength of concrete

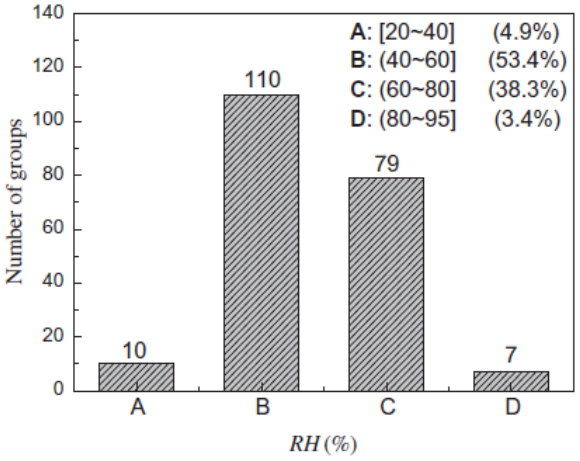

(*b*) Environmental relative humidity

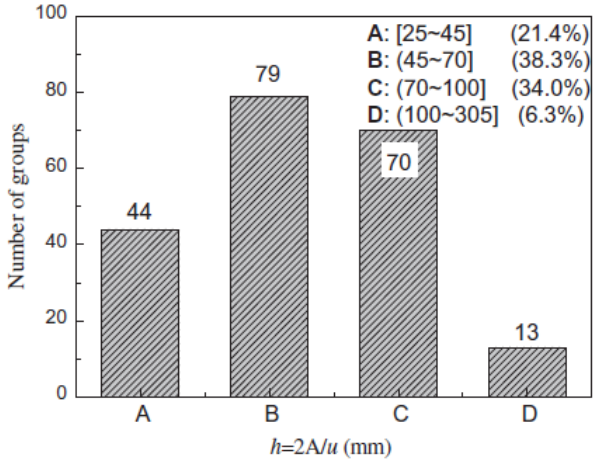

(*c*) Effective thickness to account for volume/surface ratio

Fig. 1

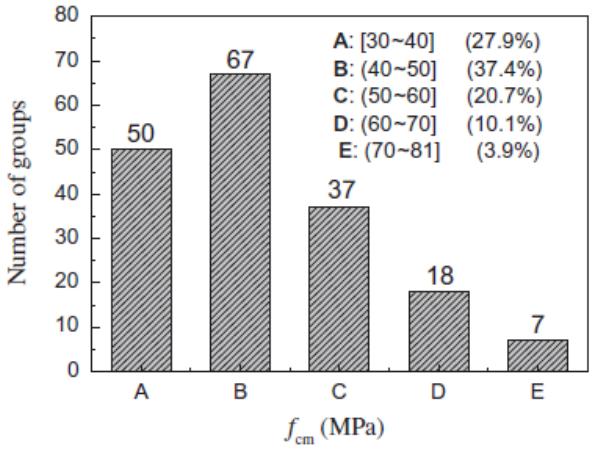

(*a*) Average 28-day compressive strength of concrete

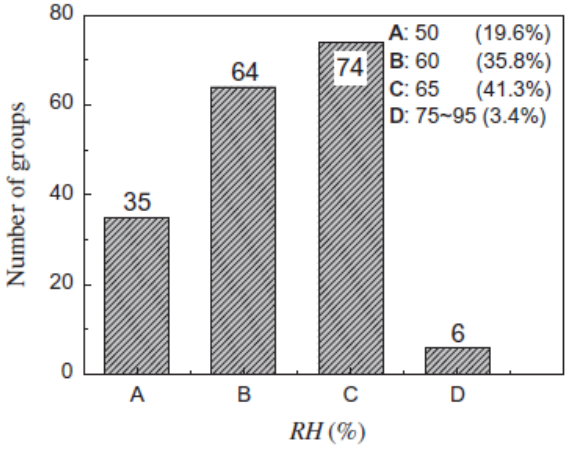

(*b*) Environmental relative humidity

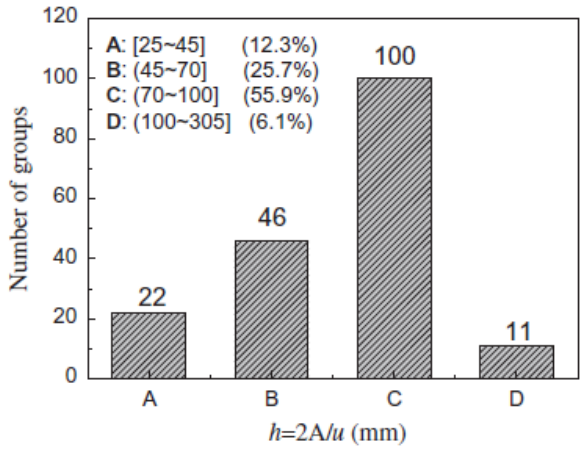

(*c*) Effective thickness to account for volume/surface ratio

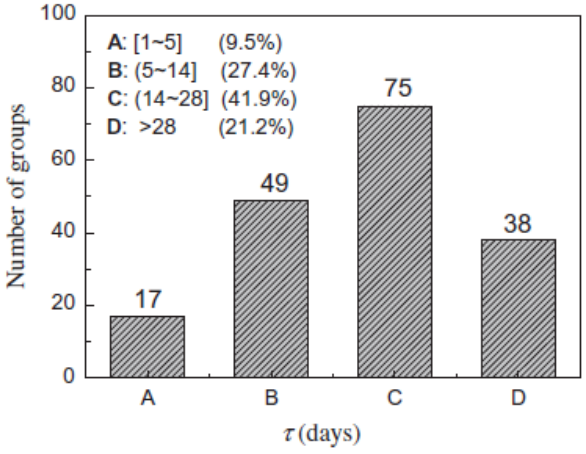

(*d*) Concrete age at loading

Fig. 2

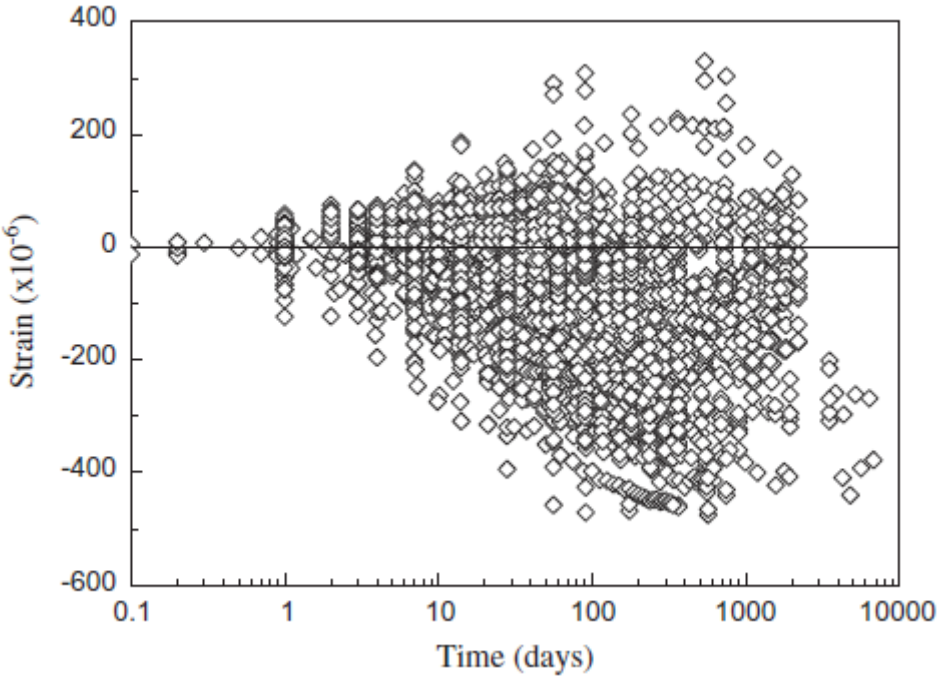
400
200
0
-200
-400
-600
Strain (x10-6)
0.1
1
10
100
1000
10000
Time (days)

Fig. 3

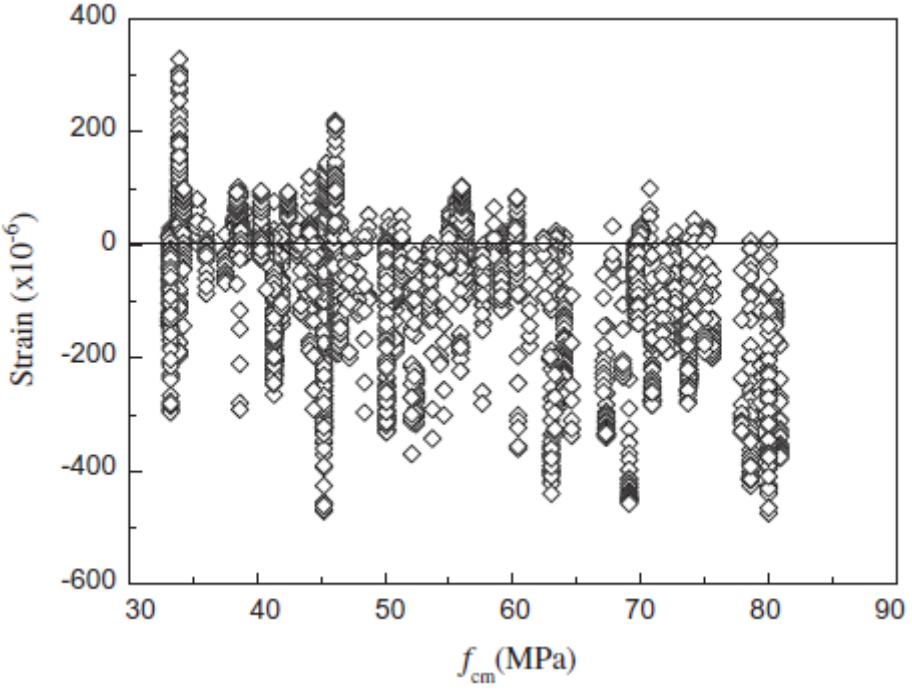

Fig. 4

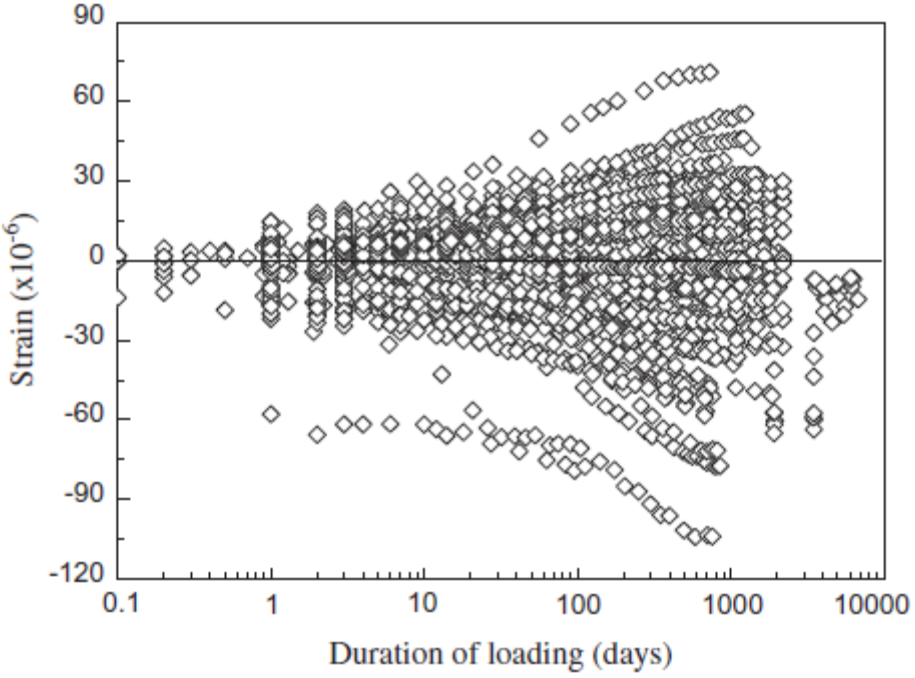
90
60
30
0
-30
-60
-90
-120
Strain (x10^{-6})
0.1
1
10
100
1000
10000
Duration of loading (days)

Fig. 5

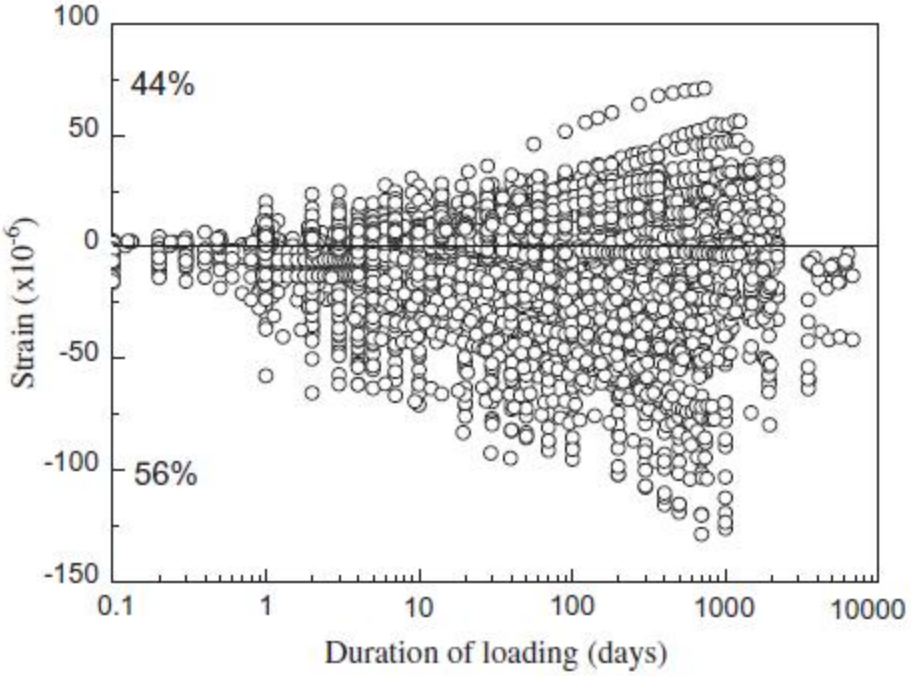
100
50
0
-50
-100
-150
44%
56%
Strain (x10^{-6})
0.1
1
10
100
1000
10000
Duration of loading (days)

Fig. 6

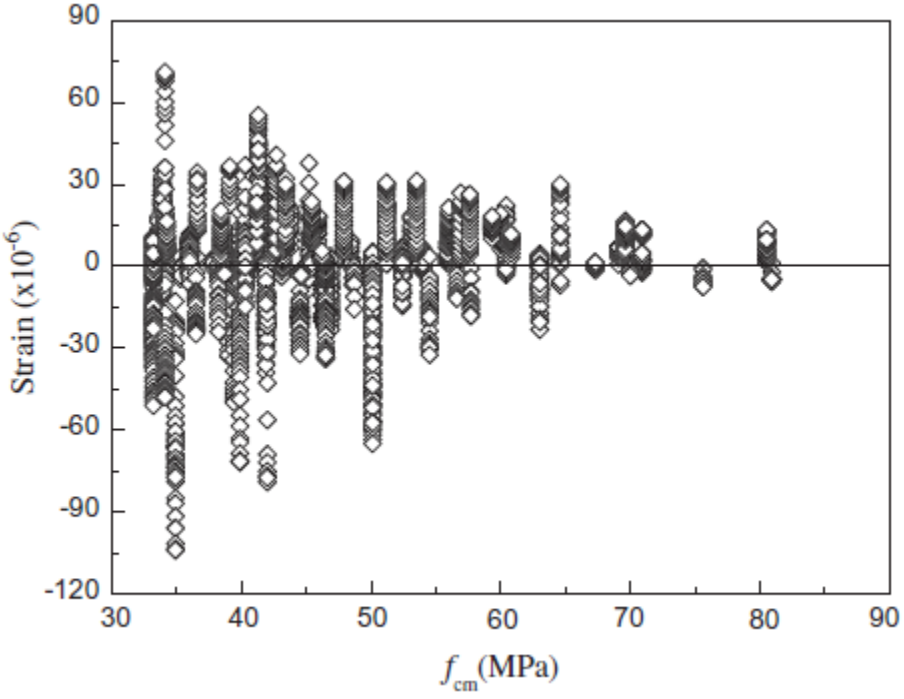

Fig. 7

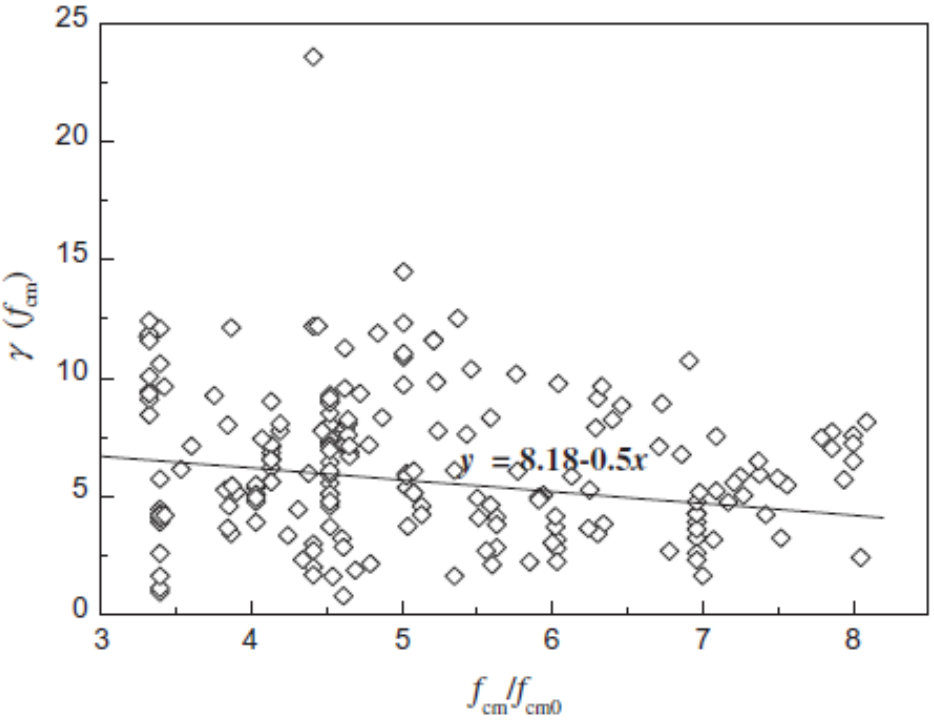

Fig. 8

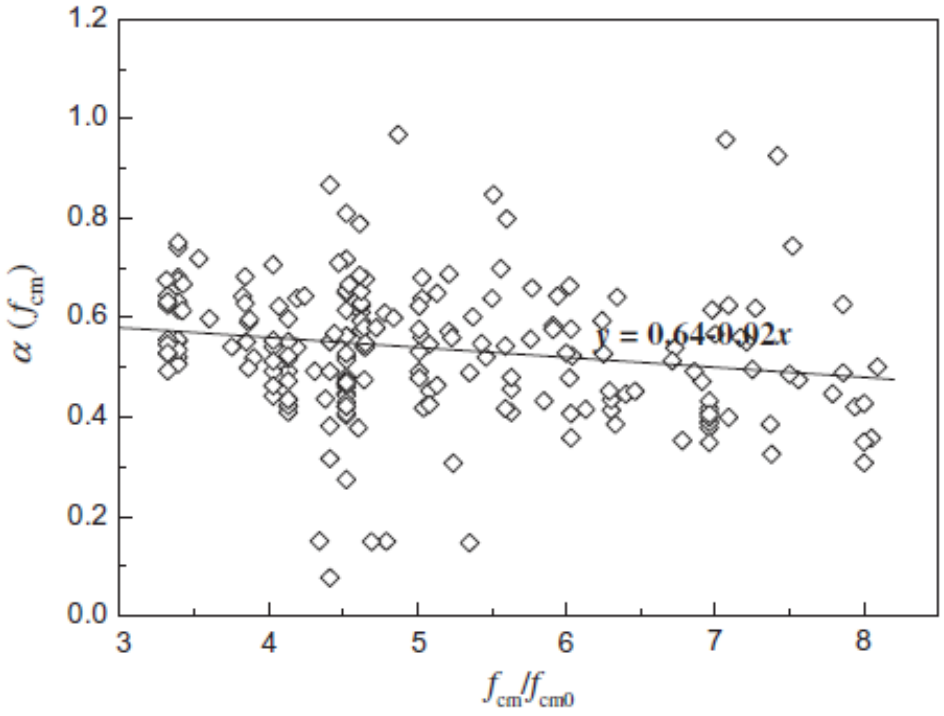

Fig. 9

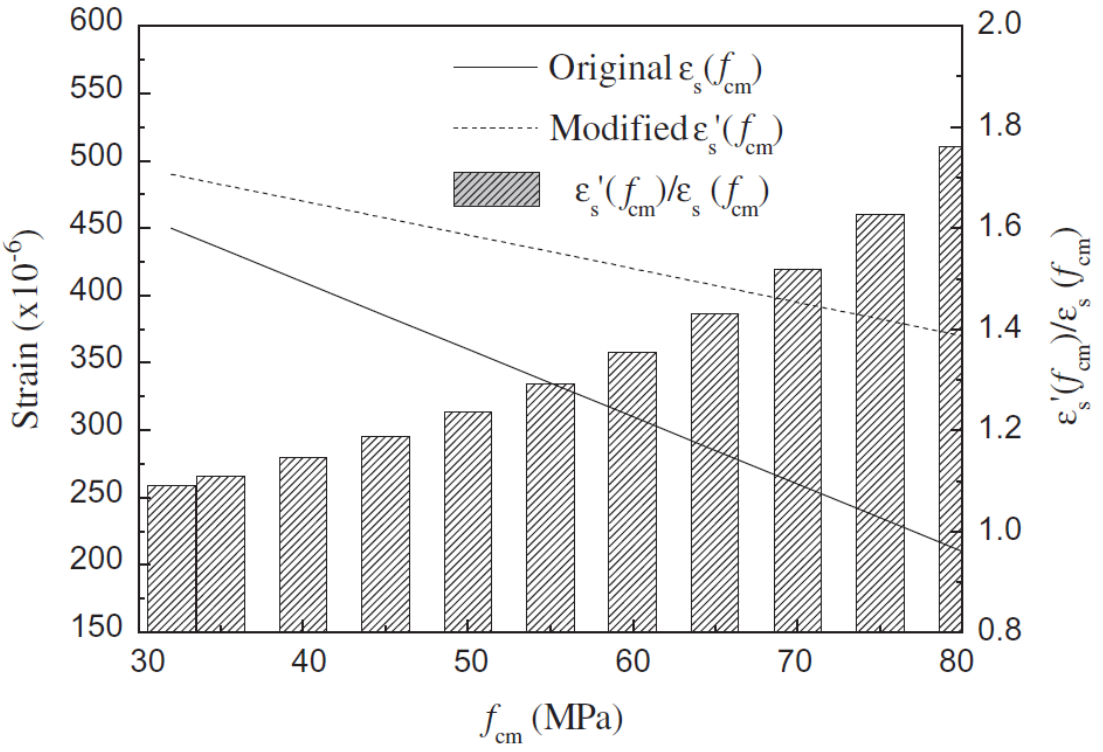
Original $\varepsilon_s(f_{cm})$
Modified $\varepsilon_s'(f_{cm})$
$\varepsilon_s'(f_{cm})/\varepsilon_s(f_{cm})$
Strain (x10^{-6})
$\varepsilon_s'(f_{cm})/\varepsilon_s(f_{cm})$
f_{cm} (MPa)
600
550
500
450
400
350
300
250
200
150
2.0
1.8
1.6
1.4
1.2
1.0
0.8
30
40
50
60
70
80

Fig. 10

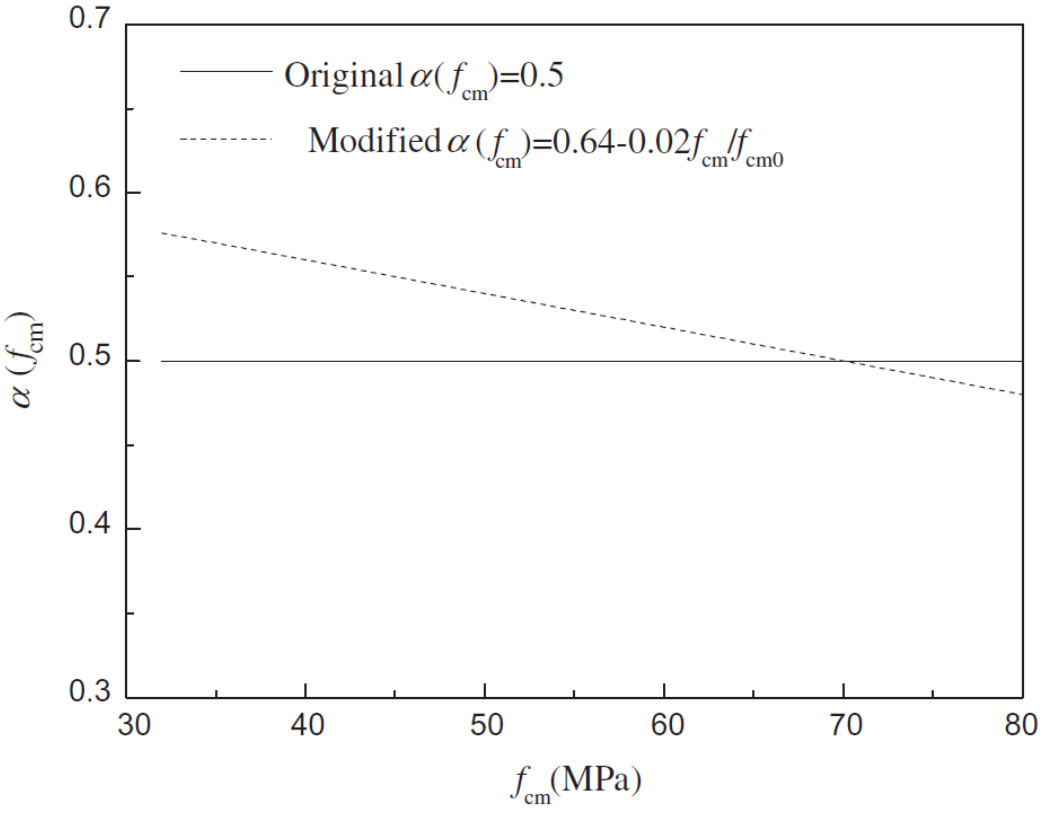
0.7
0.6
0.5
0.4
0.3
30
40
50
60
70
80
Original $\alpha(f_{cm})$=0.5
Modified $\alpha(f_{cm})$=0.64-0.02f_{cm}/f_{cm0}
$\alpha(f_{cm})$
f_{cm}(MPa)

Fig. 11

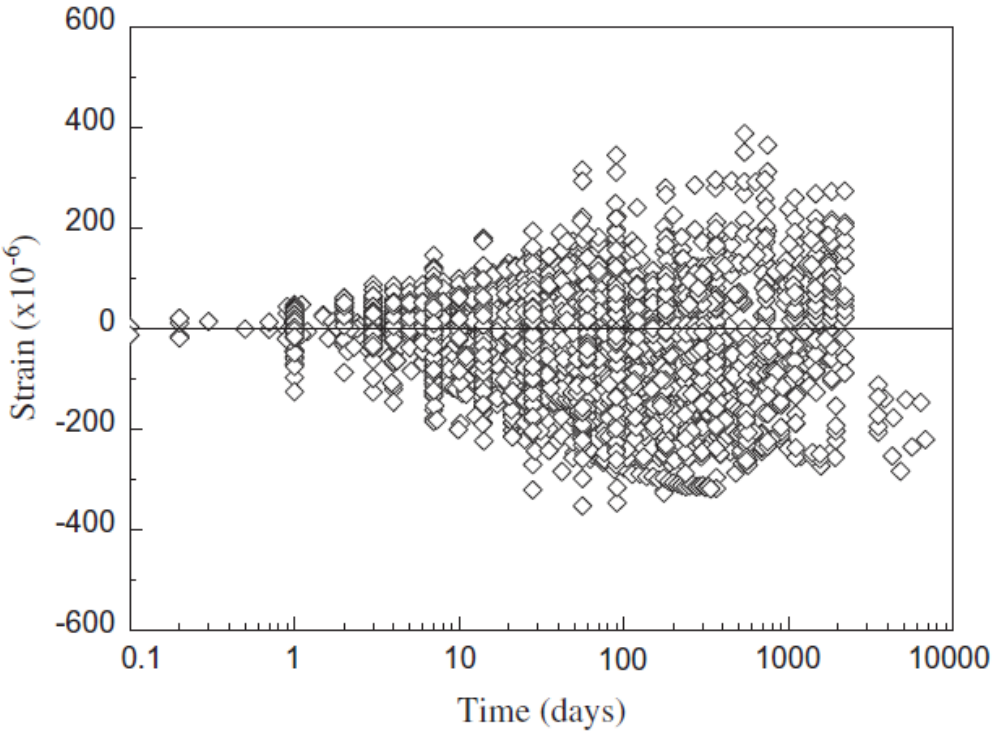
600
400
200
0
-200
-400
-600
Strain (x10-6)
0.1
1
10
100
1000
10000
Time (days)

Fig. 12

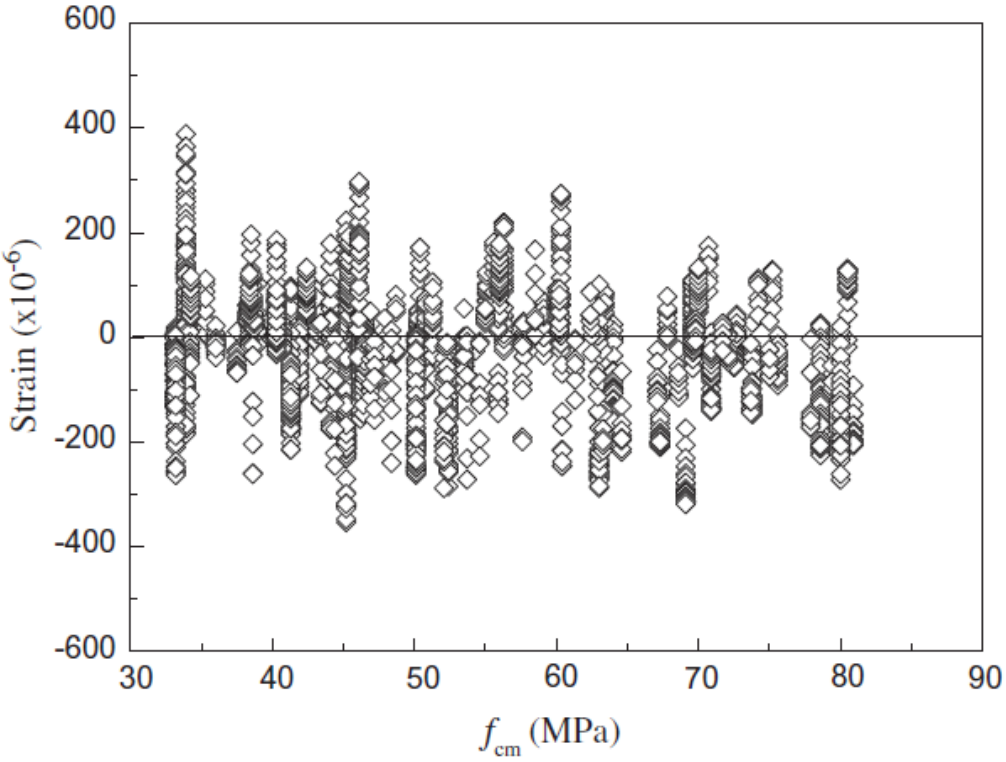

Fig. 13

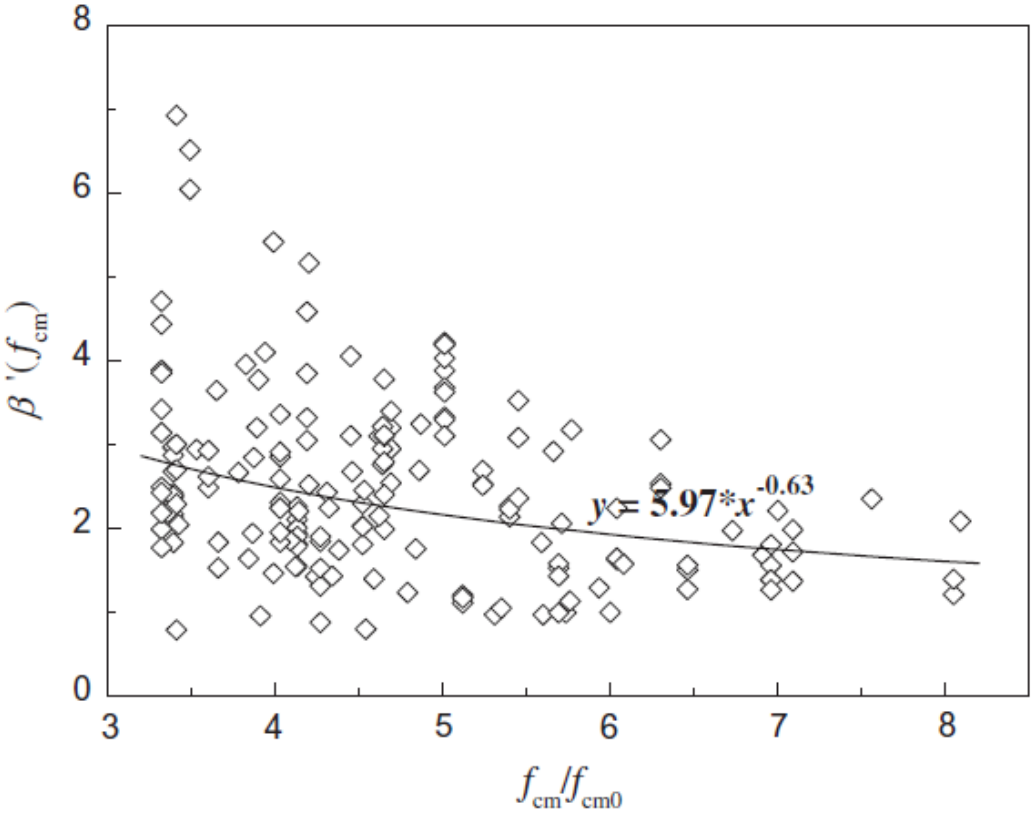

Fig. 14

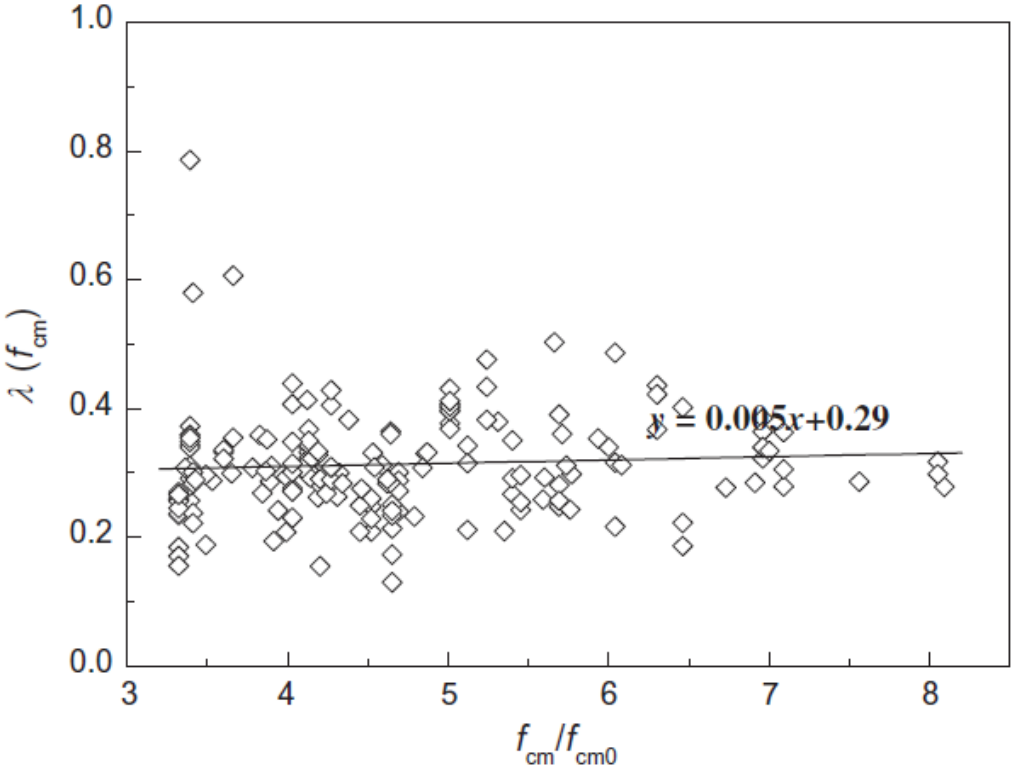

Fig. 15

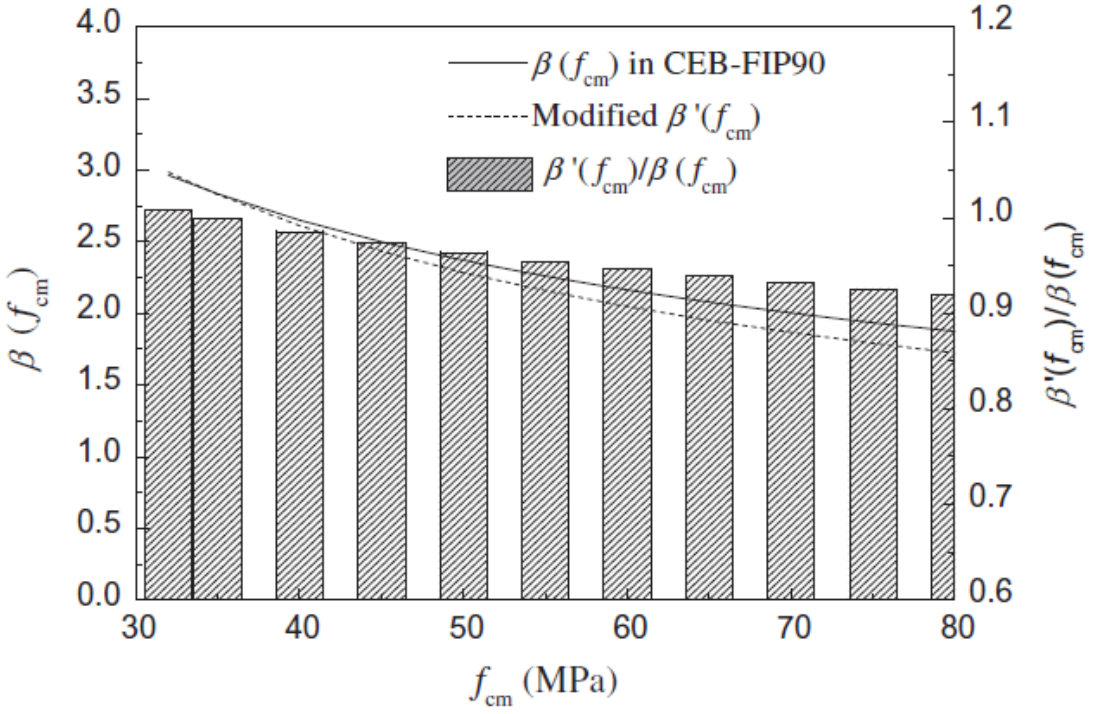
4.0
3.5
3.0
2.5
2.0
1.5
1.0
0.5
0.0
1.2
1.1
1.0
0.9
0.8
0.7
0.6
30
40
50
60
70
80
β (f_cm) in CEB-FIP90
Modified β '(f_cm)
β '(f_cm)/β (f_cm)
β (f_cm)
β'(f_cm)/β(f_cm)
f_cm (MPa)

Fig. 16

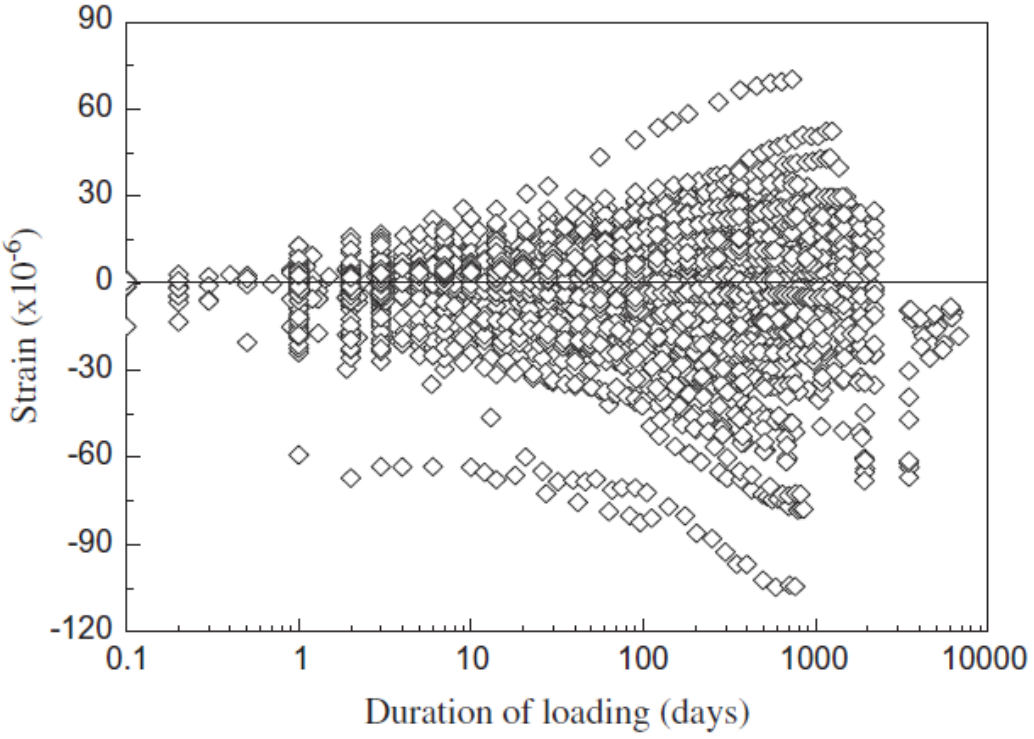
90
60
30
0
-30
-60
-90
-120
Strain (x10-6)
0.1
1
10
100
1000
10000
Duration of loading (days)

Fig. 17

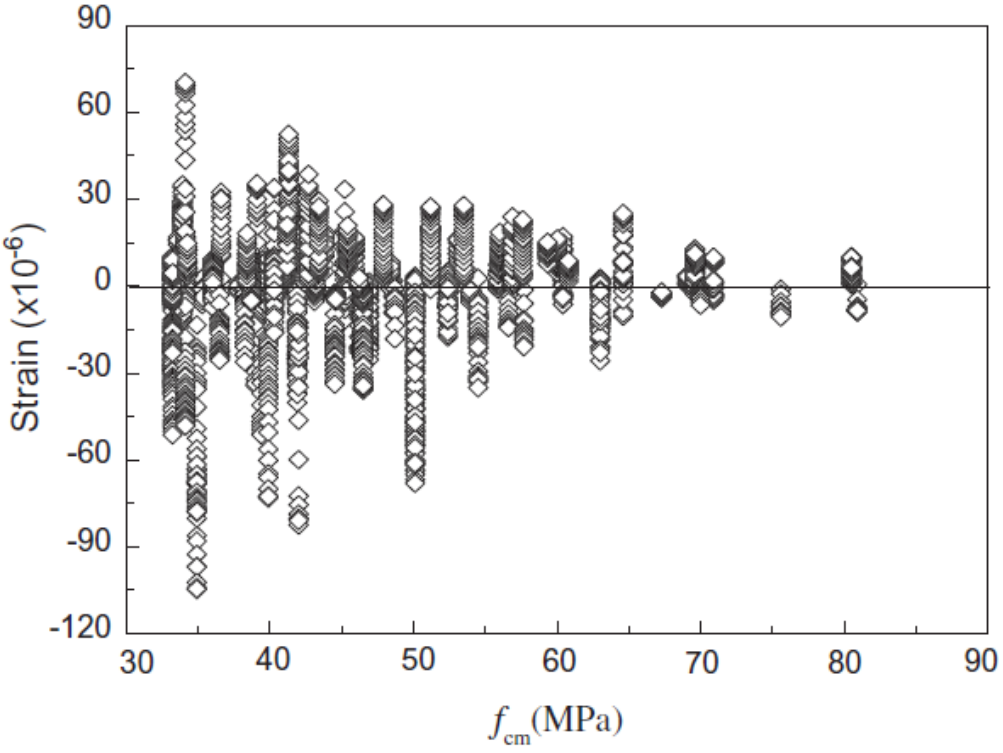

Fig. 18